Asian Journal of Chemistry; Vol. 33, No. 9 (2021), 2000-2006

ASIAN JOURNAL OF CHEMISTRY

https://doi.org/10.14233/ajchem.2021.23264

Effect of Zinc Doping on the Electrical and Dielectric Properties of CCTO Compound Synthesized by Solid-State Method

M. SLAOUI[1,2], N. GOUITAA[2], Y. EL ISSMAELI[2], A. HARRACH[1], F. ABDI[2], M. HADDAD[3] and T. LAMCHARFI[2,*]

[1]Condensed Matter Chemistry Laboratory, Sidi Mohammed Ben Abdellah University, BP 2202, Route d'Imouzzer, Faculty of Science and Technology of Fez, BP 2202, Fez, Morocco
[2]Signals, Systems and Components Laboratory, Sidi Mohammed Ben Abdellah University, BP 2202, Route d'Imouzzer, Faculty of Science and Technology of Fez, BP 2202, Fez, Morocco
[3]Materials and Archaeomaterials Spectrometry Laboratory (LASMAR), Research Unit Associated with CNRST (URAC11), Moulay-Ismail University, Faculty of Sciences, 50000 Meknès, Morocco

*Corresponding author: E-mail: lamcharfi_taj@yahoo.fr

Received: 23 April 2021; *Accepted*: 3 June 2021; *Published online*: 20 August 2021; AJC-20455

In this work, the influence of zinc doping on structural and dielectric properties of $CaCu_{(3-x)}Zn_xTi_4O_{12}$ (CCZ_xTO with x = 0, 2.5, 5, 7.5, 10, 12.5 and 15%) ceramics sintered at 1000 ºC for 8 h was studied. The ceramic samples were prepared by the conventional solid-state and calcined at 1050 ºC for 4 h. The X-ray diffraction (XRD) analysis of pure and Zn-doped CCTO were analyzed by using Rietveld refinement with cubic CCTO phase with no trace impurity phase. The scanning electron microscopy (SEM) investigation showed that for Zn-doped CCTO, the grains distributions were homogenous with average sizes which decreased with increasing of Zn concentration. The dielectric permittivity as function of temperature showed two dielectric anomalies (weakly and strong) and the dielectric constant value largely decreased for x = 2.5%, which is about tree magnitude smaller than the pure ceramic. Then it increased and reached a maximum at x = 10%, which is larger than the value of pure ceramic. And for x > 10%, the dielectric constant decreased for about two magnitude smaller than the ceramic at x = 10%. The cole-cole diagramm for all the samples showed existence of two semi-arcs attributed to the grains and grains boundaries. It was found that the R_g values were much smaller than the R_{gb} value. This give an evidance on the formation of interior barrier layer capacity (IBLC).

Keywords: Ceramic, Calcium copper titanate, Perovskite material, Dielectric properties, Doping, Complex impedance analysis.

INTRODUCTION

Perovskite materials exhibiting a giant dielectric constant with good temperature stability are widely used in industrial applications like the ceramic's capacitors and microwave devices, such as resonators and filters [1]. Among those materials, the body centered cubic perovskite material $CaCu_3Ti_4O_{12}$ (CCTO) has been extensively studied since found its extremely high dielectric response [2]. The CCTO ceramics exhibit an extraordinary colossal dielectric constant (CDC) (ε_r) of about 10^4-10^5 at room temperature which is approximately frequency and temperature stable in ranges of 10^2-10^6 Hz and 100 K to 400 K, respectively [3,4]. Theoretical studies have shown that calcium copper titanate (CCTO) ceramic has dielectric constant of about 40-50 [1,5,6]. According to these properties exhibited two opinions for describe origin of a high dielectric constant for CCTO. The first says that the CCTO is paraelectric and the origin of high dielectric constant (HDC) is attributed to extrinsic factors. While the second says the CCTO is ferroelectric and the origin is related to intrinsic factors, this problem still exists today.

This difference still exists today, in addition to several investigations which have been reported on the dielectric properties of polycrystalline and single crystal CCTO ceramics, their high loss tangent is still the most serious problem for applications based on capacitive components [7]. Many attempts have been made to understanding origin of dielectric constant and other attempts for improving the dielectric properties by reducing dielectric loss and enhancing dielectric constant with control of many factors such as processing conditions purity of raw

materials and synthesis routes aliovalent and isovalent substitutions.

The greatest tendencies for decreasing dielectric loss have been found to be along with the dielectric constant reduction [8-10]. In CCTO materials, the content of Cu has a significant influence on this dielectric property. Hadi *et al.* [11] have been dopped cobalt ($Co^{2+/3+}$) at Cu^{2+} site in CCTO material. Their results showed enhance dielectric constant and lower dielectric loss. Homes *et al.* [12] have doped Sr^{2+} at Cu^{2+} site in the CCTO material. Their results presented changes in the grain boundaries structure, which caused a reduction in the tan δ as well as a decrease in the ε_r to less than 10^4 [8]. Yang *et al.* [13] have studied Fe^{3+} at Cu^{2+} and they obtained an increase in dielectric loss and reduction in dielectric constant. There are another works by Fang & Liu [14], which have used Zn^{2+} at Cu^{2+} at concentrations of 0, 6, 10 and 20% with using sol-gel method, they obtained a decrease in the dielectric constant and dielectric loss up to 10%. Oppositely, a higher dielectric constant and dielectric loss can be observed in x = 20%. Similarly, Singh *et al.* [15] using semi while route at Zn concentrations in Cu^{2+} site at x = 0, 10, 20 and 30%, they obtained increase in the ε_r and tan δ up to x = 20%.

In this article, the effect of doping Zn^{2+} at Cu^{2+} site in CCTO according to the formula CCZ_xTO with x = 0, 2.5, 5, 7.5, 10, 12.5 and 15% is studied for samples prepared using the solid method and characterized by XRD, SEM and dielectric measurements.

EXPERIMENTAL

The solid solutions CCZ_xTO were prepared by solid state method in several steps (Fig. 1). The first step consists in preparing, by solid way, the CCTO doped with Zn by weighing the necessary quantities with stoichiometric proportions, of the following precursors: calcium carbonate , titanium oxide, copper oxide and zinc oxide. These precursors were crushed for 1 h and then milled in the presence of acetone. Placed the material in an oven at 80 ºC for 12 h. After drying, the powder was again well ground and calcined at 1050 ºC for 4 h following a thermal cycle adopted in the laboratory.

RESULTS AND DISCUSSION

XRD studies: Fig. 2 shows the X-ray diffractogram of pure and Zn-doped $CaCu_3Ti_4O_{12}$ powders calcined at 1050 ºC for 4 h. For pure CCTO, it can be observed that the sample crystallized in the pure cubic perovskite phase by compared with standard powder diffraction (JCPDF File No. 75-2188) without presence of secondary phases. The XRD patterns has been analyzed by employing Rietveld method using Full Prof Suit program [11] using $Im\bar{3}$ space group. The XRD patterns a long with Rietveld refined data has been shown in Fig. 2b and observed that the profile for calculated and observed once much well to each other and all the experimental peaks are allowed the Bragg's position for $Im\bar{3}$ space group.

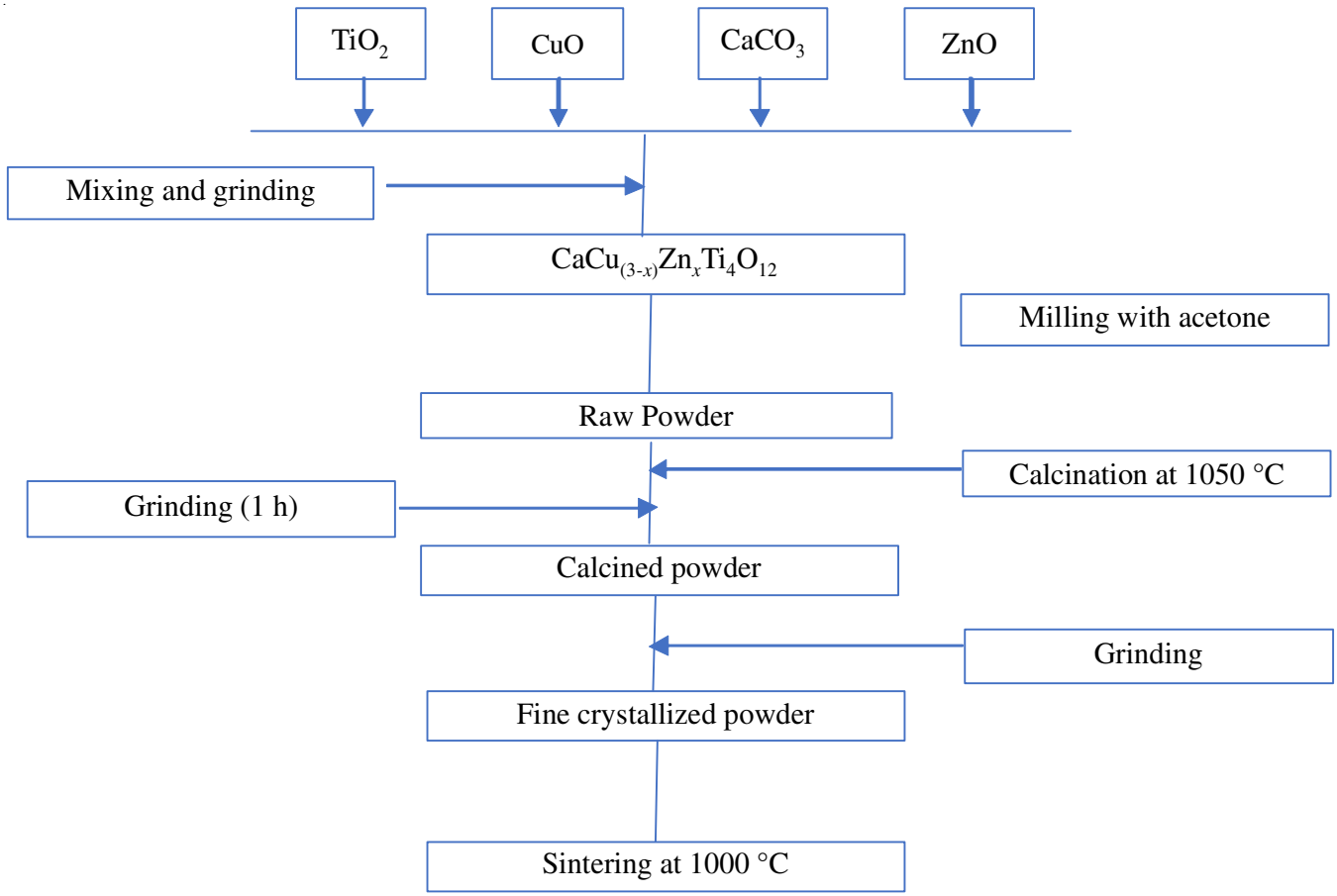

Fig. 1. Different steps of preparation of CCZ_xTO ceramic powder

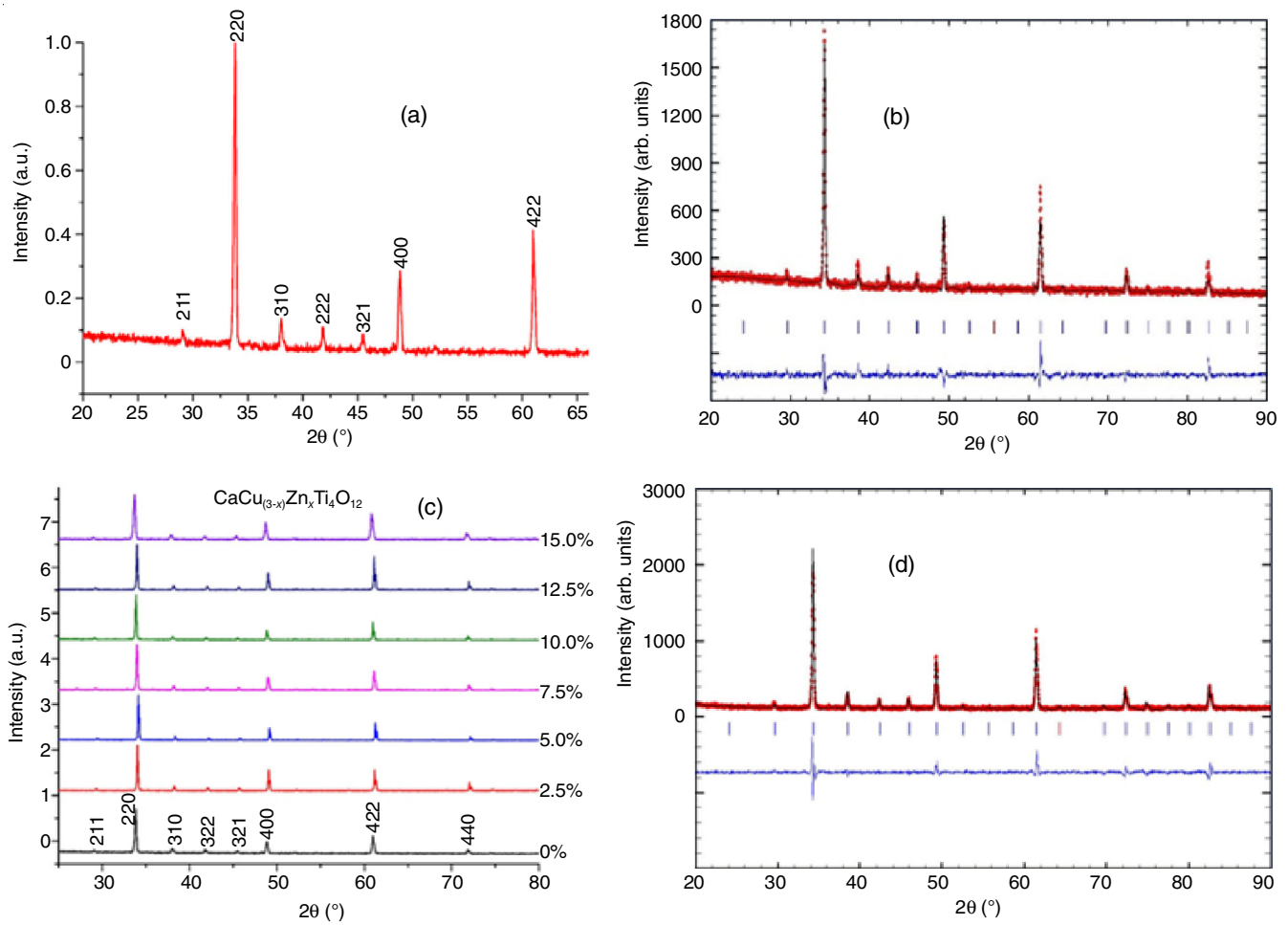

Fig. 2. (a) X-ray diffractogram of CCTO powder calcined at 1050 °C (4 h); (b) X-ray diffractogram of CCTO powder fitted by Rietveld, (c) XRD diffractogram of the different CCZ_xTO compositions (x = 0 to15 %); (d) X-ray diffractogram of the CCZ_xTO powder fitted by Rietveld

By adding Zn to CCTO for x = 0, 2.5, 5, 7.5, 10, 12.5 and 15%, the diffraction patterns show no appearance of any other peaks compared with CCTO ceramic and no trace of impurity phases as shown in Fig. 2c. We have fitted the Zn-dopped CCTO for all the samples by using Rietveld refinement, for example, sample at x = 15% as shown Fig. 2d. The fit is the same matched observed with pure phase.

The lattice parameters of pure and Zn doped CCTO were calculated and results are shown in Table-1. The lattice parameters decrease with increasing Zn substitution up to x = 7.5% then increased above this concentration, inducting that Zn maybe have good solubility in CCTO and the amount of Zn ions can replace Cu in the CCTO lattice. These results are in good agreement with the results of the literature, with a proportion that varies between 0% and 20% of zinc contents [15].

Morphology: The microstructure of CCZ_xTO ceramics sintered at 1000 ºC for 8 h is shown in Fig. 3. The SEM images of the pure CCTO ceramics is characterized by large grains with quadratic grain form separated by clear boundaries and pores. While the Zn-doped CCTO ceramics showed a change in grain form from quadratic to semi-spherical. It can also observed that the samples at x = 2.5 to 7.5% contain a homogeneous grain size. While above 7.5% of Zn content, the ceramics are constituted of both large and small grains. The average grain size decreases with increasing of zinc amount (Table-2).

TABLE-1
REFINED STRUCTURE PARAMETERS OF PURE Zn-DOPED CCTO OBTAINED BY RIETVELD

%	a = b = c (Å)	Volume (Å^3)
0	7.3852	402.7954
2.5	7.3758	401.9160
5.0	7.3742	401.0002
7.5	7.3813	402.1597
10.0	7.3867	403.0430
12.5	7.3853	402.8138
15.0	7.3885	403.3428

TABLE-2
REFINED STRUCTURE PARAMETERS OF CCZ_xTO POWDER

Rate on zinc (%)	Average grain size (µm)
0	11.71
2.5	2.78
5.0	2.25
7.5	2.07
10.0	1.96
12.5	1.75
15.0	1.74

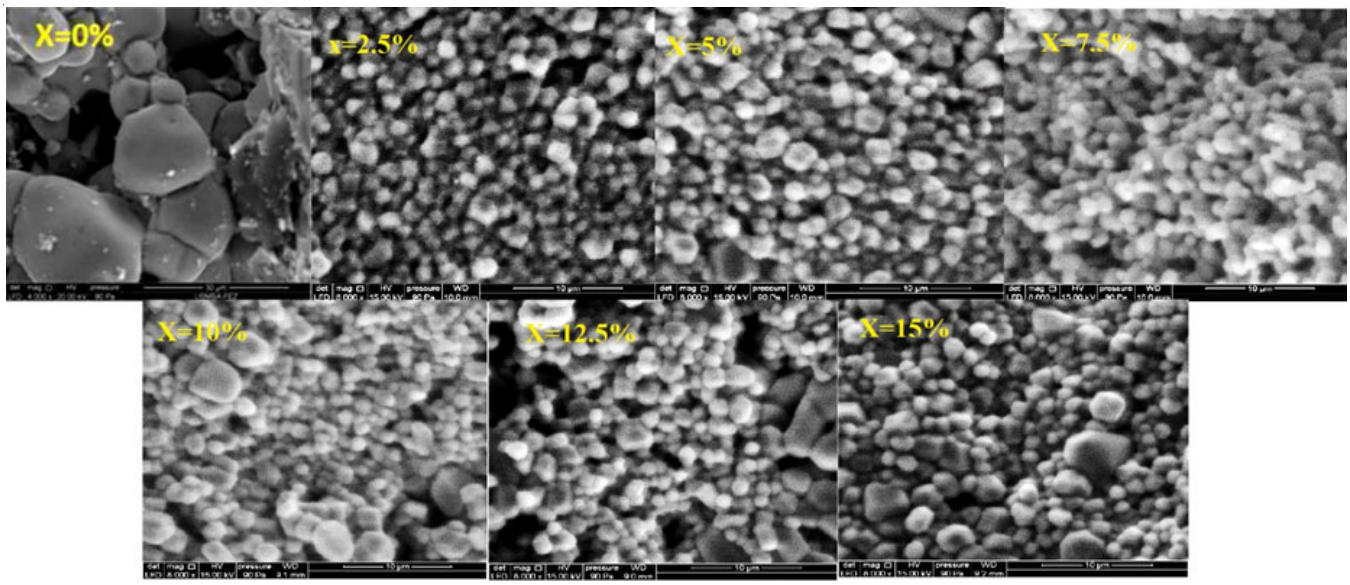

Fig. 3. SEM images of CCZ_xTO ceramics, sintered at 1000 °C for 4 h

Raman studies: The Raman spectroscopy of CCZ_xTO samples prepared by solid route calcined at 1050 ºC is shown in Fig. 4. The presence of seven modes active Raman corresponding to one A_g, two E_g and four F_g peaks were observed. All the positions of the seven lines in the Raman spectra were in a good agreement with the results predicted by the calculations of lattice dynamics [16]. The A_g, E_g and two of F_g modes are assigned to rotation-like rocking motions of TiO_6 octahedrons, while the two additional F_g modes corresponding to the breathing stretching motion of the TiO_6 octahedron and the O-Ti-O antistretching motion, respectively. The bands as Ag_1 (448 cm^{-1}), Ag_2 (511 cm^{-1}), E_g (318 cm^{-1}), Fg_1 (288 cm^{-1}) and Fg_2 (405 cm^{-1}) are classified to the rotation-like motion bands. While those at Fg_3 (579 cm^{-1}) and Fg_4 (625 cm^{-1}) corresponds to the antistretching and breathing bands, respectively [16].

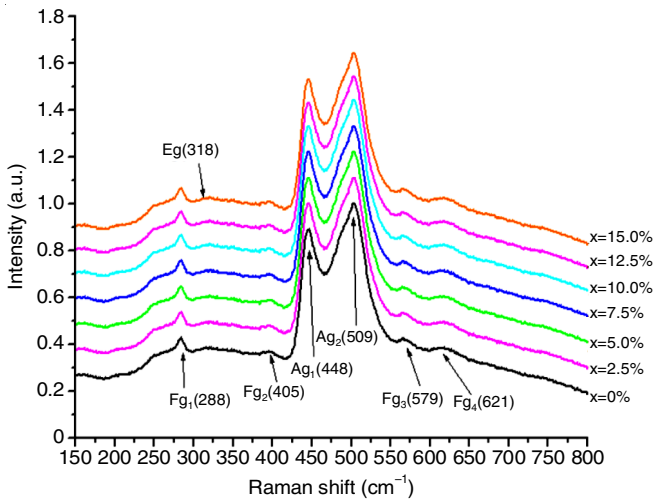

Fig. 4. Ramon spectroscopy of solid prepared CCZ_xTO powders

It can be seen that the peaks positions of all CCZ_xTO samples does not change. This indicates that zinc oxide does not affect the frequency of the modes involving O-Ti-O stretching. The same results were reported by Saîd *et al.* [17] for CCTO doped with Ni.

Dielectric studies: Fig. 5 shows the evolution of the real part of the dielectric permittivity (ε_r) of CCZ_xTO ceramics as a function of temperature at different frequencies. It is observed that ε_r value decreases with increasing frequency for all the samples. This can be explained by mechanisms of polarization that have varying time response capability to an applied field frequency [18]. For $x = 0.00$, the value of the dielectric constant increases with increasing temperature and goes through a maximum for all frequencies. While for Zn-doped CCTO ceramics, it can be cleary seen from Fig. 5, two anomalies in all samples (weakly and strong) were observed. The first (weakly peak) is observed at around 200 ºC, this peak observed in all the ceramics except at $x = 10$ and 12.5% of Zn content. At these percentage, the rapid increase of ε_r to very high values hide the appearance of this anomaly. It is also noticed that the transition temperature corresponding to this anomaly shifts to the high temperature with the increase of Zn contents. And the second strong peak is observed, at high temperature, for all the ceramics.

For the Zn-doped samples, the values of dielectric constant (Table-3) are greatly deacrease for small content of Zn (x = 2.5%), which is about tree magnitude smaller than the pure ceramic. Then the dielectric constant increase at $x = 10$ % and reached a value greater than the pur ceramic. This increase is maybe due to the relative homogeneous and/or absence of pores observed in SEM micrographs. These results are with agreement for co-doped CCTO at Ti^{4+} by Zr^{4+} and Nb^{5+} [19] and with other results for Zn doped CCTO prepared by using semiwet [15]. For samples, with x is larger than 10 %, the dielectric constant decreased to about 60 $\times 10^3$ at $x = 15\%$ which is two magnitude smaller than this of x = 10% (Table-3), this decrease maybe due to the grains fragility. These results are similar to those obtained for Cu substituted CCTO by Co [11] or by Fe [13] and the results for Zn doped CCTO ceramics prepared by using sol-gel method [14]. The comparison of present results

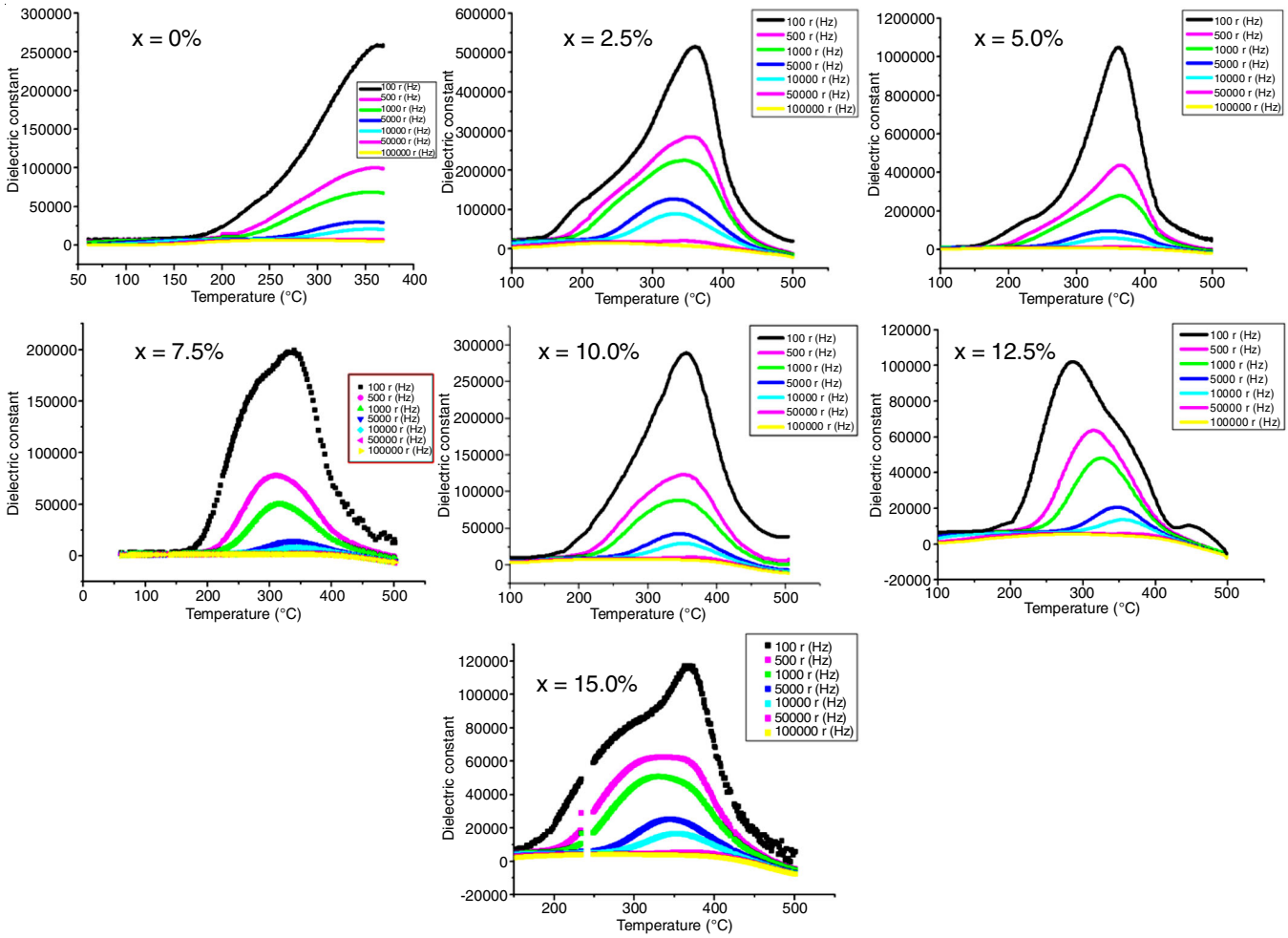

Fig. 5. Evolution of the dielectric constant, at different frequencies, as a function of temperature for CCZ_xTO (x = 0, 2.5, 5, 7.5, 10, 12.5 and 15%) sintered at 1000 °C for 4 h

TABLE-3
MAXIMUM DIELECTRIC CONSTANT AND TEMPERATURE VALUES AT 500 Hz AS A FUNCTION OF x FOR CCZ_xTO (x = 0, 2.5, 5, 7.5, 10, 12.5 AND 15%)

x (%)	ε'_{max}	Temp. (°C)
0	1002×10^3	359
2.5	2855×10^3	355
5.0	4375×10^3	365
7.5	9613×10^3	383
10.0	12263×10^3	355
12.5	6370×10^3	315
15.0	6005×10^3	393

prepared by the solid solution for pure CCTO and Zn-doped is better than the those prepared by the semiwet method [15].

The evolution of dielectric permittivity as function of frequency of CCZ_xTO ceramics, at room temperature for all the ceramics is shown in Fig. 6. This evolution shows a classical ferroelectric behaviour. However, the dielectric constant decreases with increasing frequency and becomes almost independent of frequency at high frequency region. This decrease in the dielectric constant with the increase in frequency can be explained by the phenomenon of dipole relaxation due to the contribution of interfacial polarization of the Maxwell-Wagner type [20]. The dipoles with large effective masses (*e.g.* oxygen

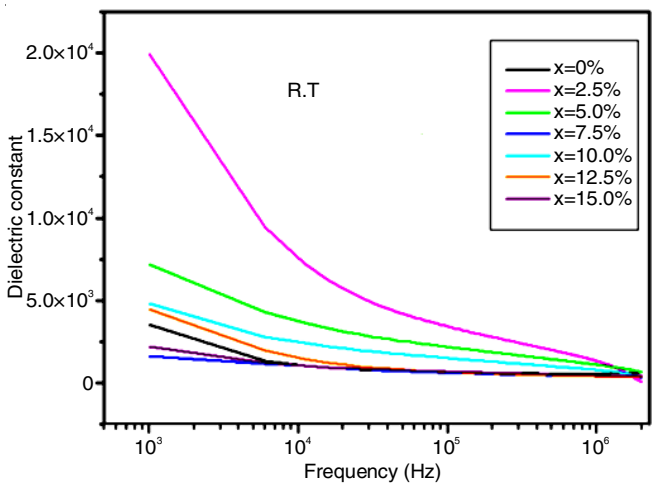

Fig. 6. Dielectric constant variation as a function frequency at different compositions for CCZ_xTO ceramics

vacancies) may follow the applied field at low frequency and does not follow it at higher frequencies.

The RT dielectric losses of the pure and Zn doped CCTO samples are shown in Fig. 7. The dielectric loss shows a frequency peak below 10^5 Hz while above this frequency range the loss increases greatly for all samples. This peak is assoc-

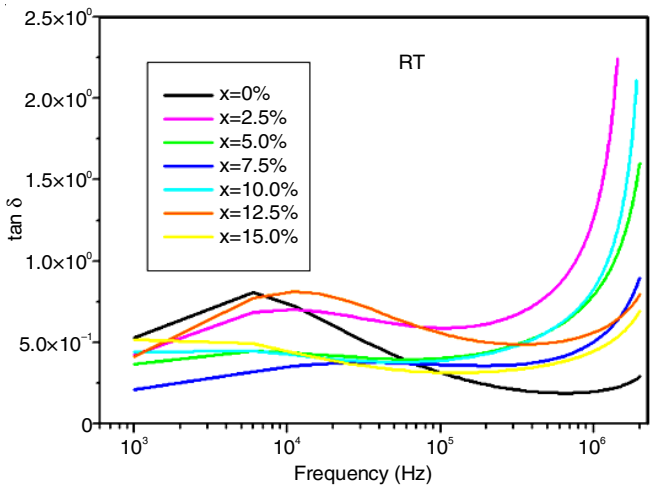

Fig. 7. Dielectric loss variation as a function frequency at different composition for CCZ_xTO at RT

iated with decrease in dielectric constant with frequency which suggested the existence of polar relaxation in all the samples.

Fig. 8 shows the conductivity dependence on the frequency at room temperature of pure and Zn dopped CCTO. As the capacitive of the sample decreases at high frequencies, the impedance decreases, resulting in an increased ac conductivity of the samples [21,22]. The results also indicated an increases in the conductivity for lower amount of Zn containts up to x = 2.5%; this may be due to oxygen vacancies concentration when increased. While at high concentration of Zn, the conduc-tivity decreases mainly in the frequency range lower than 10^5 Hz, this is related to the low carriar charge in this range. The frequency depandence of the conductivity of all the samples follows the Jonscher's power law.

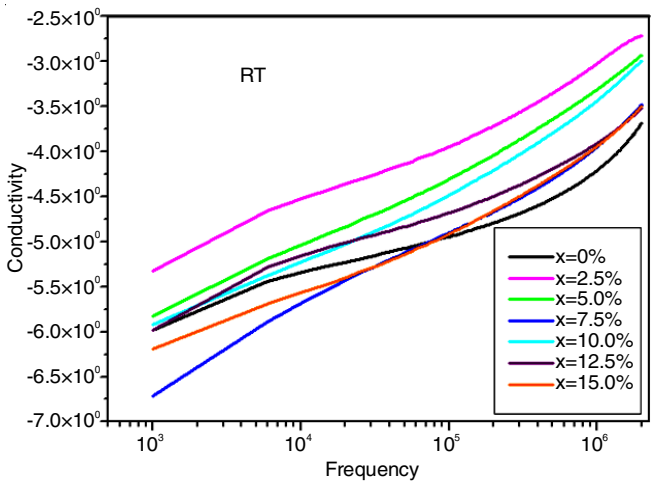

Fig. 8. Conductivity variation as a function frequency at different composition for CCZ_xT0 at RT

The complex impedance spectra analysis is regarded as a powerful method to reveal the electrically heterogeneous characteristics of CCTO ceramics [23]. The impedance components are generally considered as an equivalent circuit consisting of two parallel elements connected in series for CCTO based ceramics, representing the resistor-capacitor (RC) model correlated with the electric response of grains and grain boundary [24,25]. In present study, the samples of pure and Zn-doped CCTO at room temperature, the complex impedance spectroscopy data fitted by using the electrochemical impedance spectroscopy analysis. The plot fitted by two parallel RC as equivalent circuits connected on series (inset Fig. 9). For all the samples, it can be seen an appearance of two semi-arcs: one, is related to the grain contribution and the other antributed to the grain boundary contribution (Fig. 9). The center of all the semi-arcs is above the x-axis, which indicate a non-Debye relaxation type behaviour in these ceramics.

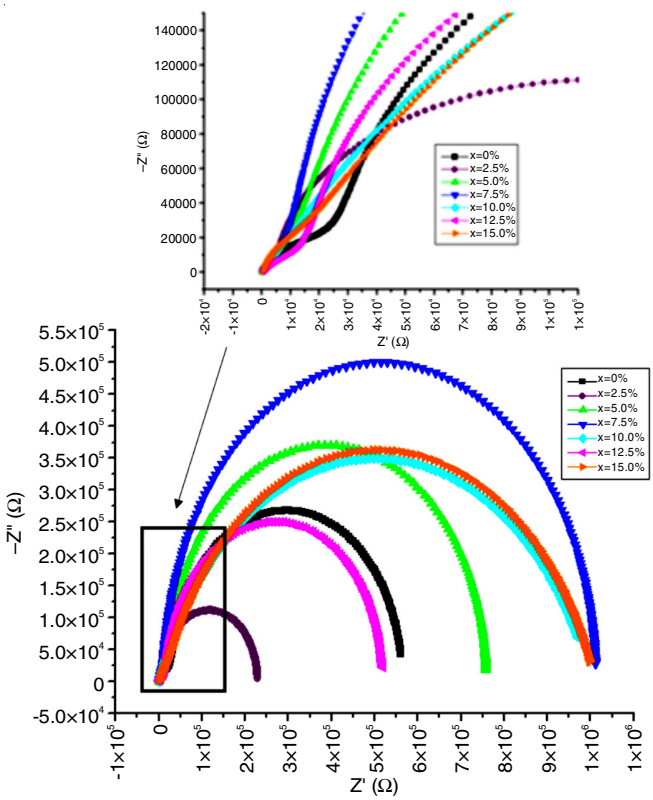

Fig. 9. Impedance analysis Z″ *vs*. Z′ of the CCZ_xTO ceramics

From the data and fitting, the grain resistance (R_g) and grain boudary resistance (R_{gb}) estimated values are given in Table-4. It can be found that the values of R_g of all samples are much smaller than the R_{gb} values. This evidence the formation of interior barrier layer capacity (IBLC). According to the IBLC model, the behaviour of $R_g << R_{gb}$ can be lead to a

TABLE-4
VALUES OF THE RESISTANCE GRAINS (R_g)
AND RESISTANCE GRAIN BOUNDARY (R_{gb})
FOR THE CCZ_xTO CERAMICS

X (%)	R_g ($\times 10^4$ Ω)	R_{gb} ($\times 10^5$ Ω)
0	2.96	5.34
2.5	6.92	2.22
5.0	2.12	7.35
7.5	1.29	10.00
10.0	1.73	10.00
12.5	1.96	4.99
15.0	9.20	10.00

large polarization at the grain boundaries and interfacial. In addition, the R_{gb} values achieve a maximum at $x = 7.5\%$ and 10%, while the R_b values are minimal at these contents.

Conclusion

In this study, the CCZ_xTO ($x = 0$, 2.5, 5, 7.5, 10, 12.5 and 15 %) ceramics were synthesized by solid state route and the effect Cu substitution Zn on the dielectric, electrical and microstructure properties of the prepared samples were investigated. The XRD diffraction showed that Zn doped CCTO did not changed the structure and phase. However, all samples crystallized in cubic phase, with $Im\bar{3}$ space group, without presence of impurity phases. The Raman spectra also confirmed the XRD results. The SEM showed a decrease in average grain sizes and an increase in homogeneity with the increase of Zn contain in CCTO. While the dielectric measurements as function of temperature show two dielectric anomalies and the dielectric constant increased with the increase in Zinc content up to $x =$ 10%. Compared with the literature, the dielectric permittivity values that obtained were higher. The conductivity results indicate an increases in the conductivity for lower amount of Zn containte up to $x = 2.5$ %. The Cole-Cole spectra showed that the values of R_g of all the samples are much smaller than those of R_{gb}, which is explained by IBLC model.

CONFLICT OF INTEREST

The authors declare that there is no conflict of interests regarding the publication of this article.

REFERENCES

1. N. Suresh Kumar and K.C. Babu Naidu, *J. Materiom.*, **7**, 940 (2021); https://doi.org/10.1016/j.jmat.2021.04.002
2. V.S. Puli, S. Adireddy, M. Kothakonda, R. Elupula and D.B. Chrisey, *J. Adv. Dielectr.*, **7**, 1750017 (2017); https://doi.org/10.1142/S2010135X17500175
3. C. Liu, P. Liu, J.-P. Zhou, Y. He, L.N. Su, L. Cao and H.-W. Zhang, *J. Appl. Phys.*, **107**, 094108 (2010); https://doi.org/10.1063/1.3359715
4. M.H. Cohen, J.B. Neaton, L.X. He and D. Vanderbilt, *J. Appl. Phys.*, **94**, 3299 (2003); https://doi.org/10.1063/1.1595708
5. C.C. Homes, T. Vogt, S.M. Shapiros, S. Wakimodo, M.A. Subramanian and A.P Ramirez, *Phys. Rev. B Condens. Matter Mater. Phys.*, **67**, 92 (2003); https://doi.org/10.1103/PhysRevB.67.092106
6. L. He, J.B. Neaton, M.H. Cohen, D. Vanderbilt and C.C. Homes, *Phys. Rev. B Condens. Matter Mater. Phys.*, **65**, 214112 (2002); https://doi.org/10.1103/PhysRevB.65.214112
7. L. Singh, U .S. Rai, K.D. Mandal and N.B. Singh, *Prog. Cryst. Growth Charact. Mater.*, **60**, 15 (2014); https://doi.org/10.1016/j.pcrysgrow.2014.04.001
8. C.-H. Mu, P. Liu, Y. He, J.-P. Zhou and H.-W. Zhang, *Alloys Compd. Rev. B*, **471**, 137 (2009); https://doi.org/10.1016/j.jallcom.2008.04.040
9. Y. Yan, L. Jin, L. Feng and G. Cao, *Sci. Eng. Rev. B*, **130**, 146 (2006); https://doi.org/10.1016/j.mseb.2006.02.060
10. D. Xu, K. He, R. Yu, X. Sun, Y. Yang, H. Xu, H. Yuan and J. Ma, *J. Mater. Chem. Phys. Rev. B*, **153**, 229 (2015); https://doi.org/10.1016/j.matchemphys.2015.01.007
11. N. Hadi, F. Abdi, T. Lamcharfi, N.S. Echtoui, A. Harrach, M. Zouhairi and F. Ahjyaje, *Mediterranean J. Chem.*, **8**, 234 (2009); https://doi.org/10.13171/mjc8319052011nh
12. C.C. Homes, T. Vogt, S.M. Shapiro, S. Wakimoto and A.P. Ramirez, *Science*, **293**, 673 (2001); https://doi.org/10.1126/science.1061655
13. Z. Yang, Y. Zhang, G. You, K. Zhang, R. Xiong and J. Shi, *J. Mater. Sci. Technol. Rev. B*, **28**, 1145 (2012); https://doi.org/10.1016/S1005-0302(12)60184-4
14. T.-T. Fang and C.P. Liu, *J. Chem. Mater.*, **17**, 5167 (2005); https://doi.org/10.1021/cm051180k
15. L. Singh, U.S. Rai and K.D. Mandal, *Appl. Phys. A*, **112**, 891 (2013); https://doi.org/10.1007/s00339-012-7443-z
16. D. Valim, A.G. Souza Filho, P.T.C. Freire, S.B. Fagan, A.P. Ayala, J. Mendes Filho, A.F.L. Almeida, P.B.A. Fechine, A.S.B. Sombra, J. Staun Olsen and L. Gerward, *Phys. Rev. B Condens. Matter Mater. Phys.*, **70**, 132103 (2004); https://doi.org/10.1103/PhysRevB.70.132103
17. S. Saîd, S. Didry, M. El Amrani, C. Autret-lambert and A. Megriche, *J. Alloys Compd.*, **765**, 927 (2018); https://doi.org/10.1016/j.jallcom.2018.06.282
18. T.-T. Fang and L.-T. Mei, *J. Am. Ceram. Soc.*, **90**, 638 (2007); https://doi.org/10.1111/j.1551-2916.2006.01419.x
19. P. Mao, J. Wang, P. Xiao, L. Zhang, F. Kang and H. Gong, *Ceram. Int.*, **47**, 111 (2021); https://doi.org/10.1016/j.ceramint.2020.08.113
20. Z. Yu and C. Ang, *J. Appl. Phys. B*, **91**, 794 (2002); https://doi.org/10.1063/1.1421033
21. L. Singh, U.S. Rai, A.K. Rai and K.D. Mandal, *Electron. Mater. Lett.*, **9**, 107 (2013); https://doi.org/10.1007/s13391-012-2095-x
22. G. Li, Z. Chen, X. Sun, L. Liu, L. Fang and B. Elouadi, *Mater. Res. Bull.*, **65**, 260 (2015); https://doi.org/10.1016/j.materresbull.2015.02.012
23. P. Pokhriyal, A. Bhakar, A.K. Sinha and A. Sagdeo, *J. Appl. Phys.*, **125**, 164101 (2019); https://doi.org/10.1063/1.5064483
24. P. Mao, J. Wang, S. Liu, L. Zhang, Y. Zhao and L. He, *J. Alloys Compd.*, **778**, 625 (2019); https://doi.org/10.1016/j.jallcom.2018.11.200
25. J.T.S. Irvine, D.C. Sinclair and A.R. Wes, *Adv. Mater.*, **2**, 132 (1990); https://doi.org/10.1002/adma.19900020304